



C. H. MARCHI, C. R. MALISKA & A. F. C. SILVA  
 Department of Mechanical Engineering  
 Federal University of Santa Catarina  
 P.O. Box 476 - 88049 - Florianópolis, SC, Brazil



SUMMARY

The solution of three dimensional compressible flow problems defined in arbitrary geometries requires the use of generalized coordinates in order to have flexibility in handling complex geometries. The use of segregated finite-volume methods requires special procedure to deal with the pressure-velocity coupling, involving, in general, staggered grids for promoting strenght to the coupling. Unfortunately the use of staggered grids introduces several difficulties in the computer code implementation. In this work a 3D numerical model is developed employing co-located variables for the solution of all speed flows.

INTRODUCTION

The majority of the existing numerical methods and computer codes for solving high speed compressible fluid flow problems belongs to the class of methods which employs the state equation for the pressure determination and the mass conservation equation for density calculation. It is well reported, however, that for low Mach number flows these methods are no longer suitable [1]. The other class of methods is the one where the density is determined from the state equation and pressure is found through an special equation derived using the mass conservation constraint. These methods are suitable for solving incompressible fluid flow problems or problems where the density is a function of temperature only. It is known that the development of the former class of methods occurred among the aerospace numerical analysts while the latter class develop among the analysts involved with incompressible flow. It is illustrative to report some important differences between these two classes of methods. The former class of methods employ higher order finite-difference schemes using co-located variables, while the methods in the latter class employ the staggered grid arrangement, to cope with the pressure-velocity coupling, and derive the algebraic equations involving the conservation principles at control volume level, being called finite volume methods.

Very recently, extensions of the methodologies employed for incompressible flows have been applied with success in the solution of compressible fluid flow problems in cartesian [2,3] and general coordinate systems [4,5]. These methods form an equation for pressure, replacing, in the mass conservation equation, density by a linearized form of the state equation and velocity components by their respective momentum equations. The drawback of these methods is that they require the use of staggered variables in order to provide the adequate coupling between pressure and velocity/density. As a consequence of the staggered arrangement the computer code implementation becomes cumbersome, specially if variable grid spacing is used in three dimensions, because the different control volume locations and the corresponding metric storing.

The alternative to this problem is to keep all variables stored at the same point, that is, all of them share the same elemental control volume. The use of co-located variables simplifies considerably the coefficients calculation and storing, and geometrical data storing. The difficulty associated with the use of co-located variables is the poor coupling it provides between pressure and

velocity/density. This difficulty can be removed taking care in numerically approximating the pressure gradients.

Successful applications of finite volume methods for 2D problems using nonorthogonal grids with co-located variables can be seen in [6,7] for incompressible flows, in [8], among others, for cartesian grids and 2D incompressible flows, in [3] for 2D compressible flows in cartesian grids and in [4,5,9] for 2D compressible flows in general curvilinear coordinates.

The very good results obtained in [3,4,5,9] encouraged the authors the development of a numerical scheme using co-located variables for the solution of 3D flows. The method can solve compressible flow with presence of strong shocks as well as incompressible fluid flow problems, due to the special linearization performed for the mass flux in the mass conservation equation.

The development of such a method is the main purpose of the present paper. The model advances the state of the art in the solution of 3D all speed flows using co-located variables in the context of finite volume methods. Preliminary results, which demonstrates the aplicability of the method are also presented. It is believed that the development here in presented is in the direction of obtaining powerful, easy to implement and general numerical methods for the solution of all speed flows.

GOVERNING EQUATIONS

The Euler equations written for a general coordinate system  $(\xi, \eta, \gamma)$  for a generic scalar  $\phi$  are

$$\frac{1}{J} \frac{\partial}{\partial t}(\rho\phi) + \frac{\partial}{\partial \xi}(\rho U\phi) + \frac{\partial}{\partial \eta}(\rho V\phi) + \frac{\partial}{\partial \gamma}(\rho W\phi) + \hat{p}\phi = 0 \quad (1)$$

The  $\phi$  variable represents the mass conservation equation, the three cartesian velocity components and the energy equation, being equal to 1, u, v, w and T, respectively. A state equation, as below, closes the system of equations which governs the three-dimensional flow of an inviscid fluid.

$$p = \rho RT \quad (2)$$

The Jacobian of the transformation and the contravariant velocity components appearing in Eq.(1)

are given by

$$J = [X_{\xi} Y_{\eta} Z_{\gamma} + X_{\eta} Y_{\gamma} Z_{\xi} + X_{\gamma} Y_{\xi} Z_{\eta} - X_{\xi} Y_{\gamma} Z_{\eta} - X_{\eta} Y_{\xi} Z_{\gamma} - X_{\gamma} Y_{\eta} Z_{\xi}]^{-1} \quad (3)$$

$$U = u \bar{\xi}_X + v \bar{\xi}_Y + w \bar{\xi}_Z \quad (4)$$

$$V = u \bar{\eta}_X + v \bar{\eta}_Y + w \bar{\eta}_Z \quad (5)$$

$$W = u \bar{\gamma}_X + v \bar{\gamma}_Y + w \bar{\gamma}_Z \quad (6)$$

where

$$\bar{\xi}_X = Z_{\gamma} Y_{\eta} - Z_{\eta} Y_{\gamma} \quad \bar{\eta}_X = Z_{\xi} Y_{\gamma} - Z_{\gamma} Y_{\xi}$$

$$\bar{\xi}_Y = Z_{\eta} X_{\gamma} - Z_{\gamma} X_{\eta} \quad \bar{\eta}_Y = Z_{\gamma} X_{\xi} - Z_{\xi} X_{\gamma}$$

$$\bar{\xi}_Z = Y_{\gamma} X_{\eta} - Y_{\eta} X_{\gamma} \quad \bar{\eta}_Z = Y_{\xi} X_{\gamma} - Y_{\gamma} X_{\xi} \quad (7)$$

$$\bar{\gamma}_X = Z_{\eta} Y_{\xi} - Z_{\xi} Y_{\eta} \quad \bar{\gamma}_Z = Y_{\eta} X_{\xi} - Y_{\xi} X_{\eta}$$

$$\bar{\gamma}_Y = Z_{\xi} X_{\eta} - Z_{\eta} X_{\xi}$$

The source term,  $\hat{p}^{\phi}$ , in this case involving only the pressure field, for the three momentum conservation equations and for the energy equation are given below. For the mass conservation, of course,  $\hat{p}^{\phi}$  is equal to zero.

$$\hat{p}^u = \left[ \frac{\partial p}{\partial \xi} \bar{\xi}_X + \frac{\partial p}{\partial \eta} \bar{\eta}_X + \frac{\partial p}{\partial \gamma} \bar{\gamma}_X \right] \quad (8)$$

$$\hat{p}^v = \left[ \frac{\partial p}{\partial \xi} \bar{\xi}_Y + \frac{\partial p}{\partial \eta} \bar{\eta}_Y + \frac{\partial p}{\partial \gamma} \bar{\gamma}_Y \right] \quad (9)$$

$$\hat{p}^w = \left[ \frac{\partial p}{\partial \xi} \bar{\xi}_Z + \frac{\partial p}{\partial \eta} \bar{\eta}_Z + \frac{\partial p}{\partial \gamma} \bar{\gamma}_Z \right] \quad (10)$$

$$\hat{p}^T = -\frac{1}{c} \frac{1}{J} \left[ \frac{\partial p}{\partial t} + \nabla \cdot (p \vec{v}) - p \cdot \nabla \vec{v} \right] \quad (11)$$

#### DISCRETIZATION OF THE MOMENTUM AND ENERGY EQUATIONS

The algebraic equations are obtained employing the finite-volume method, that is, by integration of Eq.(1) over the elemental control volume shown in Fig.1 and integration in time. The resulting equation has the form

$$\begin{aligned} & (M_P \phi_P - M_P^0 \phi_P^0) / \Delta t + \dot{M}_e \phi_e - \dot{M}_w \phi_w + \dot{M}_n \phi_n \\ & - \dot{M}_s \phi_s + \dot{M}_d \phi_d - \dot{M}_f \phi_f + L[\hat{p}^{\phi}]_P \Delta \xi \Delta \eta \Delta \gamma = 0 \quad (12) \end{aligned}$$

The subscripts e, w, n, s, d and f, appearing in the equations indicate the interface of the control volume of Fig. 1, while the subscripts E, W, N, S, D and F indicate the P neighbouring control volumes. For simplicity the dimensions of the elemental control volume in the transformed space,  $\Delta \xi$ ,  $\Delta \eta$  and  $\Delta \gamma$  are

taken equal to unity. In Eq.(12)  $M_P$  and  $M_P^0$  represent the mass inside the control volume in the time  $t+\Delta t$  and  $t$ , respectively.  $\dot{M}$  is the mass flux at the interface indicated by the subscript.  $L[\hat{p}^{\phi}]$  represents the numerical approximation of the term  $\hat{p}^{\phi}$ . In this paper  $\hat{p}^{\phi}$  is approximated by the Central Differencing Scheme (CDS) [10]. To illustrate  $L[\hat{p}^u]$  is given by

$$L[\hat{p}^u]_P = \frac{(p_E - p_W)}{2\Delta \xi} (\bar{\xi}_X)_P + \frac{(p_N - p_S)}{2\Delta \eta} (\bar{\eta}_X)_P + \frac{(p_D - p_F)}{2\Delta \gamma} (\bar{\gamma}_X)_P \quad (13)$$

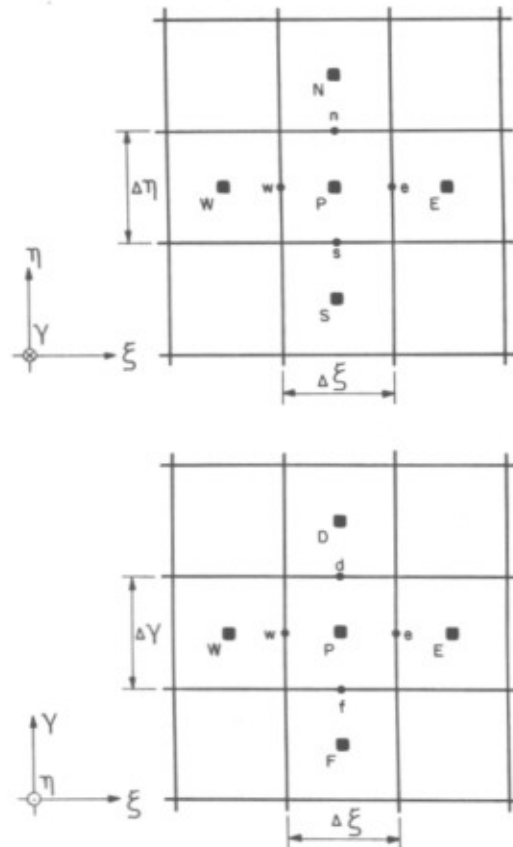


Fig. 1 Elemental control volume for P.

As the problem under consideration does not involve diffusive terms, evaluating the convective fluxes at the control volume interfaces through the Upstream Differencing Scheme (UDS) [10], the final discretized form of Eq.(1) is

$$a_P \phi_P = \sum (a_{nb} \phi_{NB})_P + M_P^0 \phi_P^0 / \Delta t - L[\hat{p}^{\phi}]_P \Delta \xi \Delta \eta \Delta \gamma \quad (14)$$

where

$$a_P = M_P^0 / \Delta t + \sum a_{nb}$$

$$\sum a_{nb} = a_e + a_w + a_n + a_s + a_d + a_f$$

$$\sum (a_{nb} \phi_{NB})_P = a_e \phi_E + a_w \phi_W + a_n \phi_N + a_s \phi_S + a_d \phi_D + a_f \phi_F$$

$$\begin{aligned}
 a_e &= - (1/2 - \bar{\alpha}_e) \dot{M}_e & a_w &= (1/2 + \bar{\alpha}_w) \dot{M}_w \\
 a_n &= - (1/2 - \bar{\alpha}_n) \dot{M}_n & a_s &= (1/2 + \bar{\alpha}_s) \dot{M}_s \\
 a_d &= - (1/2 - \bar{\alpha}_d) \dot{M}_d & a_f &= (1/2 + \bar{\alpha}_f) \dot{M}_f
 \end{aligned} \quad (15)$$

Of course, for the Euler equations, the parameter  $\bar{\alpha}$  assumes the value +1/2 and -1/2 depending on the signal of the velocity at the interface under consideration. Since the implicit formulation is adopted, Eq.(14) originates a linear system for each dependent variable  $u$ ,  $v$ ,  $w$  and  $T$ . Recall that the coefficients of Eq.(14) are identical for  $u$ ,  $v$ ,  $w$  and  $T$  since the co-located arrangement of variables is employed.

#### DISCRETIZATION OF THE MASS CONSERVATION EQUATION

The method used in this work for finding pressure is an extension of the methodologies used in the solution of incompressible flows, that is, the mass conservation equation is transformed in an equation for pressure or pressure correction.

In the solution of compressible flows  $\rho$  and velocity are expressed in terms at pressure and substituted into the mass conservation equation forcing both density and velocity be active in this equation [2,10,11,12].

The discretized form of the mass conservation equation is obtained integrating this equation over space and time, giving

$$(\dot{M}_p - \dot{M}_p^0)/\Delta t + \dot{M}_e - \dot{M}_w + \dot{M}_n - \dot{M}_s + \dot{M}_d - \dot{M}_f = 0 \quad (16)$$

where  $\dot{M}_e$ , for example is expressed by

$$\dot{M}_e = (\rho_e^* U_e + \rho_e U_e^* - \rho_e^* U_e^*) \Delta \eta \Delta \gamma \quad (17)$$

It is seen by Eq.(17) that the velocity components which enters the mass conservation equation are the contravariant ones.

The key question now is to replace the mass fluxes as a function of pressure. Since in the mass flux calculation  $\rho$  and velocity are involved, both  $\rho$  and velocity need to be written as a function of pressure. Following the SIMPLEX [13] procedure to handle the pressure/velocity/density coupling the velocity and density are written as

$$\rho = \rho^* + \rho' \quad \vec{V} = \vec{V}^* + \vec{V}' \quad (18)$$

where the corrections in  $\rho^*$  and  $\vec{V}^*$  must be such that mass is conserved. The equation for  $\vec{V}$  transforms in three scalar equations for the  $U$ ,  $V$  and  $W$  contravariant velocity components. The star represents values from the previous iteration level, and the prime values need to be related to a pressure correction  $p'$  related to pressure by  $p = p^* + p'$ .

Density as a Function of  $p'$ . To obtain the relation between density and  $p'$  the state equation is linearized as

$$\rho = \rho^* + C^p \cdot p' \quad (19)$$

where

$$C^p = 1/RT \quad (20)$$

for the special case of the fluid being a perfect gas.

Velocity Components as a Function of  $p'$ . The expressions for the contravariant velocity components as a function at  $p'$  are obtained from the momentum conservation equations. Consider that if a correct pressure field is introduced in the conservation equations it gives rise to correct  $u$ ,  $v$  and  $w$  cartesian velocity components, and if a guessed pressure field  $p^*$  is introduced it gives rise to a estimated  $u^*$ ,  $v^*$  and  $w^*$  velocities. Subtracting the equations one obtains, for exemple, for the  $u_e$  cartesian velocity component

$$u_e = u_e^* - \bar{d}_p^U \cdot L[p^*]_e \Delta \xi \quad (21)$$

The parameter  $\bar{d}_p^U$  changes according to the pressure/velocity coupling method used. Using the above velocity components the expression for the contravariant component can be obtained as

$$U_e = U_e^* - \bar{d}_p^U \cdot (p'_E - p'_P) \cdot (\alpha_{11})_e \quad (22)$$

Similar equations can be written for the other five components which enters the mass conservation equation. In order to avoid a 19-point equation for  $p'$  the pressure gradients in the direction other than that of the velocity in consideration are neglected. For the SIMPLEX [13] method used here the expression for the  $\bar{d}_p^U$  is

$$\bar{d}_p^U = (1/2) \cdot (d_p + d_E) \Delta \eta \Delta \gamma \quad (23)$$

where

$$d_p = [a_p - \sum a_{nb}]^{-1} \quad (24)$$

Since the above equation is a velocity correction equation its form does not alter the converged results. Different equations influences only the convergence rate but not the final results.

Equation for  $p'$ . Introducing Eq.(19) and Eq.(22) for all densities and velocities which enter mass conservation in Eq.(16) with their mass flux terms linearized by Eq.(17), the resulting equation is an equation for  $p'$  in the form

$$A_p p'_p = \sum (A_{nb} p'_{nb}) + B \quad (25)$$

where

$$\begin{aligned}
 A_p = & m_p^p C_p^p + m_e^U d_p^U (\alpha_{11})_e - m_w^U d_w^U (\alpha_{11})_w + m_n^{V-V} d_n^V (\alpha_{22})_n \\
 & - m_s^{V-V} d_s^V (\alpha_{22})_s + m_d^W d_p^W (\alpha_{33})_d - m_f^W d_f^W (\alpha_{33})_f
 \end{aligned}$$

$$B = \rho_p^0 \frac{\Delta\xi\Delta\eta\Delta\gamma}{J_p\Delta t} - m_p^{\rho p} - m_e^{\rho e} - m_w^{\rho w} \\ - m_n^{\rho n} - m_s^{\rho s} - m_d^{\rho d} - m_f^{\rho f}$$

$$\{\sum A_{nb} p'_{NB}\} = A_e p'_E + A_w p'_W + A_n p'_N + A_s p'_S + A_d p'_D + A_f p'_F \quad (26)$$

$$A_e = -m_e^{\rho C} + m_e^{U-U}(\alpha_{11})_e \quad A_w = -m_w^{\rho C} - m_w^{U-U}(\alpha_{11})_w \\ A_n = -m_n^{\rho C} + m_n^{V-V}(\alpha_{22})_n \quad A_s = -m_s^{\rho C} - m_s^{V-V}(\alpha_{22})_s \\ A_d = -m_d^{\rho C} + m_d^{W-W}(\alpha_{33})_d \quad A_f = -m_f^{\rho C} - m_f^{W-W}(\alpha_{33})_f$$

and

$$\alpha_{11} = (\bar{\xi}_x)^2 + (\bar{\xi}_y)^2 + (\bar{\xi}_z)^2$$

$$\alpha_{22} = (\bar{\eta}_x)^2 + (\bar{\eta}_y)^2 + (\bar{\eta}_z)^2$$

$$\alpha_{33} = (\bar{\gamma}_x)^2 + (\bar{\gamma}_y)^2 + (\bar{\gamma}_z)^2$$

$$m_p^{\rho} = \frac{\Delta\xi\Delta\eta\Delta\gamma}{J_p\Delta t} + (1/2 + \bar{\beta}_e)U_e^* \Delta\eta\Delta\gamma - (1/2 - \bar{\beta}_w)U_w^* \Delta\eta\Delta\gamma \\ + (1/2 + \bar{\beta}_n)V_n^* \Delta\xi\Delta\gamma - (1/2 - \bar{\beta}_s)V_s^* \Delta\xi\Delta\gamma \\ + (1/2 + \bar{\beta}_d)W_d^* \Delta\xi\Delta\eta - (1/2 - \bar{\beta}_f)W_f^* \Delta\xi\Delta\eta$$

$$m_e^{\rho} = (1/2 - \bar{\beta}_e)U_e^* \Delta\eta\Delta\gamma \quad m_w^{\rho} = - (1/2 + \bar{\beta}_w)U_w^* \Delta\eta\Delta\gamma$$

$$m_n^{\rho} = (1/2 - \bar{\beta}_n)V_n^* \Delta\xi\Delta\gamma \quad m_s^{\rho} = - (1/2 + \bar{\beta}_s)V_s^* \Delta\xi\Delta\gamma$$

$$m_d^{\rho} = (1/2 - \bar{\beta}_d)W_d^* \Delta\xi\Delta\eta \quad m_f^{\rho} = - (1/2 + \bar{\beta}_f)W_f^* \Delta\xi\Delta\eta$$

$$m_e^U = [(1/2 + \bar{\beta}_e)\rho_p^* + (1/2 - \bar{\beta}_e)\rho_E^*] \Delta\eta\Delta\gamma \quad (27)$$

$$m_n^V = [(1/2 + \bar{\beta}_n)\rho_p^* + (1/2 - \bar{\beta}_n)\rho_N^*] \Delta\xi\Delta\gamma$$

$$m_d^W = [(1/2 + \bar{\beta}_d)\rho_p^* + (1/2 - \bar{\beta}_d)\rho_D^*] \Delta\xi\Delta\eta$$

$$m_w^U = - [(1/2 + \bar{\beta}_w)\rho_w^* + (1/2 - \bar{\beta}_w)\rho_p^*] \Delta\eta\Delta\gamma$$

$$m_s^V = - [(1/2 + \bar{\beta}_s)\rho_s^* + (1/2 - \bar{\beta}_s)\rho_p^*] \Delta\xi\Delta\gamma$$

$$m_f^W = - [(1/2 + \bar{\beta}_f)\rho_f^* + (1/2 - \bar{\beta}_f)\rho_p^*] \Delta\xi\Delta\eta$$

where the  $\bar{\beta}$  coefficients are evaluated in the same way as the  $\bar{a}$  coefficients of Eq.(15).

#### THE STAR CONTRAVARIANT VELOCITIES AT THE INTERFACES

As is known the dependent variables in the momentum equations are the cartesian velocity

components  $u$ ,  $v$  and  $w$ . Since one is using co-located variables the  $u$ ,  $v$  and  $w$  velocities are all stored at the center of the control volumes. In order to obtain an adequate coupling between pressure and velocity the correction equations which enters the mass conservation equation need to be written using velocities at the interfaces. However, there is no velocities stored at the interfaces. It is necessary, then to compute the star contravariant velocities at the interfaces as a function of the star cartesian velocities located in the center of the control volumes.

The PVF-A procedure to compute  $U^*$ ,  $V^*$  and  $W^*$  at the interfaces is described in [3] for cartesian grids and in [4] for general curvilinear grids and is akin to Peric's [8] procedure for incompressible flows.

Taking as an example the calculation of  $U$  at the east face, one recognizes that  $u^*$ ,  $v^*$  and  $w^*$  are needed at the east face. Writing Eq.(14) for the variable  $u$  for the control volume  $P$  for an estimated pressure field  $p^*$ , one gets

$$u_p^* = \frac{[\sum (a_{nb} u_{NB}^*)_P + M_P^0 u_P^0 / \Delta t]}{(a_p)_P} - \frac{\Delta\xi\Delta\eta\Delta\gamma}{(a_p)_P} \cdot L[p^* u]_P \quad (28)$$

and for the E control volume

$$u_E^* = \frac{[\sum (a_{nb} u_{NB}^*)_E + M_E^0 u_E^0 / \Delta t]}{(a_p)_E} - \frac{\Delta\xi\Delta\eta\Delta\gamma}{(a_p)_E} \cdot L[p^* u]_E \quad (29)$$

The velocity  $u^*$  at the east face using the PVF-A approach is obtained through the average of  $u_p^*$  and  $u_E^*$ , with exception of the pressure term, resulting in

$$u_e^* = \frac{[\sum (a_{nb} u_{NB}^*)_P + \sum (a_{nb} u_{NB}^*)_E + (M_P^0 u_P^0 + M_E^0 u_E^0) / \Delta t]}{[(a_p)_P + (a_p)_E]} \\ - \frac{2\Delta\xi\Delta\eta\Delta\gamma}{[(a_p)_P + (a_p)_E]} \cdot L[p^* u]_e \quad (30)$$

The  $L[p^* u]_e$  appearing in Eq.(30) is the numerical approximation of  $\hat{p}^u$  as if the control volume were centered in "e". The expression for  $L[p^* u]_e$  is

$$L[p^* u]_e = \frac{(p_E^* - p_P^*)}{\Delta\xi} (\bar{\xi}_x)_e + \frac{(p_N^* + p_{NE}^* - p_S^* - p_{SE}^*)}{4\Delta\eta} (\bar{\eta}_x)_e \\ + \frac{(p_D^* + p_{DE}^* - p_F^* - p_{FE}^*)}{4\Delta\gamma} (\bar{\gamma}_x)_e \quad (31)$$

The cartesian velocity components  $v^*$  and  $w^*$  at the same interface are obtained in the same manner. Knowing  $u_e^*$ ,  $v_e^*$  and  $w_e^*$  the  $U_e^*$  contravariant component can be calculated. The calculation of the remaining contravariant components follows the same procedure.

Velocity Corrections Using  $p'$ . The contravariant components are corrected using Eq.(22), for  $U$ , and using similar equations for  $V$  and  $W$ . These corrected velocities will be used for computing the coefficients for the next iteration level. The cartesian velocity components are corrected using the  $p'$  field by

$$\begin{aligned}
 u_p &= u_p^* - d_p \cdot L[\hat{p}'^u]_p \Delta \xi \Delta \eta \Delta \gamma \\
 v_p &= v_p^* - d_p \cdot L[\hat{p}'^v]_p \Delta \xi \Delta \eta \Delta \gamma \\
 w_p &= w_p^* - d_p \cdot L[\hat{p}'^w]_p \Delta \xi \Delta \eta \Delta \gamma
 \end{aligned}
 \tag{32}$$

Recall that the resulting expressions for  $L[\hat{p}'^\phi]$  are the same as for  $L[\hat{p}^\phi]$  replacing  $p$  by  $p'$ ,

#### SOLUTION PROCEDURE

The significant steps during the solution procedure now follow:

1. Domain discretization.
2. Estimative of  $u, v, w, T, p$  and  $\rho$  in  $t+\Delta t$ .
3. Computation of the coefficients and source term of the momentum equations. Solve for  $u^*, v^*$  and  $w^*$  using MSI [14] technique. Computation of the contravariant velocities at the interfaces of the control volumes.
4. Solve for  $p'$  using MSI. Compute  $p = p^* + p'$ .
5. Correction of  $u^*, v^*$  and  $w^*$ , using Eq. (32), of  $U^*, V^*$  and  $W^*$  using Eq.(22) and similar equations and correction of density using Eq.(19).
6. Solution of  $T$  using MSI. Computation of  $\rho$  using the state equation.
7. Iteration is necessary until convergence for the time step under consideration is reached.

#### PRELIMINARY RESULTS

The preliminary tests of the numerical method was realized solving four high speed flow problems. The first one aimed to test the invariance characteristic of a 2D plane flow along the axis of the cylinder, by solving the flow problem over a circular cylinder. In the direction of the cylinder axis three cells were used, with the total grid being  $26 \times 20 \times 3$ . The results (not present here) show excellent agreement when compared with the 2D solution using  $26 \times 20$  elemental volumes.

The second problem, with the objective of testing the symmetry characteristics of a 2D axisymmetric flow, was the flow over the nose tip of the Brazilian Launch Vehicle (VLS), with angle of attack ( $\alpha$ ) equal to zero and Mach number equal to 3.75. With  $\alpha$  equal to zero the solution can be compared with the 2D axisymmetric solution. In this case the number of volumes in the axisymmetric direction can not be smaller as enough for applying boundary conditions, as in the 2D plane case, because the number of volumes defines the shape of the revolution body. Two grids with  $30 \times 24 \times 10$  and  $30 \times 24 \times 20$  were used. The results are shown in Fig. 2 where the triangles denote the experimental solution [15], curve 1 shows the 2D axisymmetric results ( $30 \times 24$ ) [5], curve 2 the 3D solution with  $30 \times 24 \times 10$  and curve 3 the solution with  $30 \times 24 \times 20$  volumes. It can be seen that the results with a more refined grid in the angular direction tends to the experimental results.

The third test was the solution of the VLS vehicle, again with  $\alpha = 0$  and Mach number 3.75 but extending the computational domain up to half of the third launching stage. Fig. 3 shows the results where the triangles are the experimental results [15] and the solid line the 3D numerical solution using  $60 \times 24 \times 20$  volumes distributed in  $180^\circ$ , which is equivalent of using  $60 \times 24 \times 40$  volumes.

The final test present here is the solution of the same flow as in the third test but with  $\alpha = 5^\circ$ , characterizing the flow as truly three-dimensional. The results of pressure coefficient ( $C_p$ ) over the surface for  $\theta = 90^\circ, 160^\circ$  and  $230^\circ$  are presented in

Fig. 4, where the triangles represents the experimental results for  $\alpha = 0$ . The numerical solutions were obtained using a convergence criterion in the pressure [4] of  $10^{-5}$ , and  $2 \times 10^{-5}$ , for these second, third and last test, respectively. The fully 3D problem was not solved to a tighter convergence due solely to computer limitations.

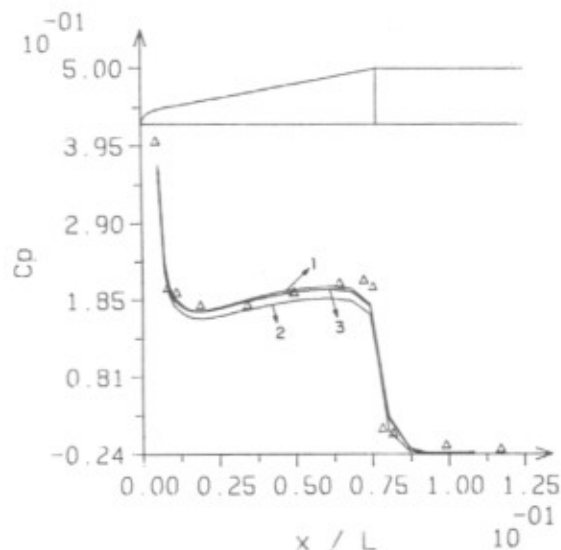


Fig. 2 Test of the symmetry characteristics.

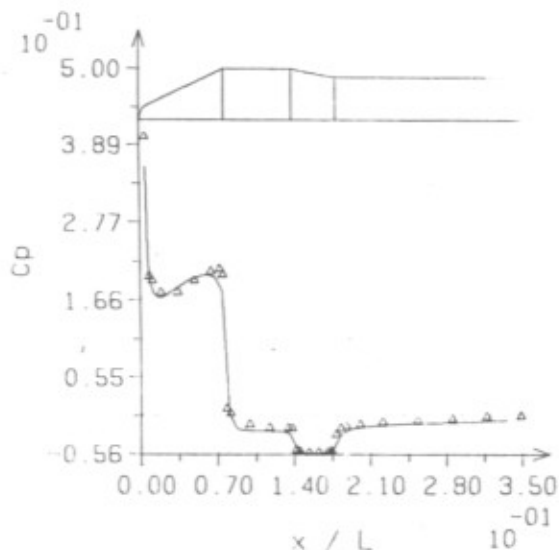


Fig. 3  $C_p$  for Mach 3.75 and  $\alpha = 0^\circ$ .

#### CONCLUDING REMARKS

The development of a 3D numerical model for the solution of all speed flows using co-located variable was described. The model incorporates two important features, namely, the possibility of solving flows ranging from low speed incompressible flows to compressible supersonic flows, and the use of co-located variables which introduces a tremendous simplicity in the code implementation when compared with the usual staggered grid. The model is also tailored to handle complex arbitrary geometries. The preliminary tests demonstrated that the method performs very well.

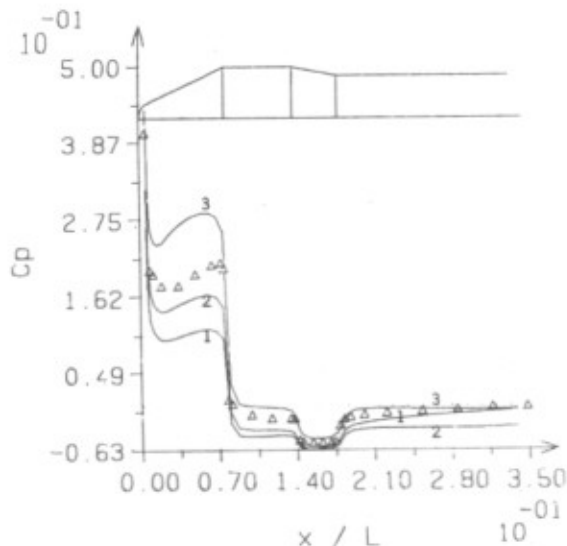


Fig. 4 Cp for Mach 3.75 and  $\alpha = 50^\circ$ .

#### ACKNOWLEDGMENTS

The partial financial support provided by Instituto de Atividades Espaciais IAE/CTA is gratefully acknowledged.

#### REFERENCES

- [ 1 ] Anderson, D.A., Tannehill, J.C. and Pletcher, R.H., "Computational Fluid Mechanics and Heat Transfer," McGraw-Hill, Washington, 1984.
- [ 2 ] Van Doormaal, J.P., "Numerical Methods for the Solution of Incompressible and Compressible Fluid Flows," Ph.D. Thesis, University of Waterloo, Ontario, Canada, 1985.
- [ 3 ] Marchi, C.H., Maliska, C.R. and Bortoli, A.L., "The Use of Co-Located Variables in the Solution of Supersonic Flows," Proceedings of the 10th Brazilian Congress of Mechanical Engineering, Vol. 1, pp. 157-160, Rio de Janeiro, Brazil, 1989.
- [ 4 ] Marchi, C.H. and Maliska, C.R., "The Use of Co-Located Variables in the Solution of Supersonic Flows," Submitted to Numerical Heat Transfer, 1990.
- [ 5 ] Maliska, C.R., Silva, A.F.C. and Marchi, C.H. "Solução Numérica de Escoamentos Compressíveis Utilizando-se Variáveis Co-Localizadas em Coordenadas Generalizadas," Relatório ao IAE/CTA, parte 5, Florianópolis, SINMEC/EMC/UFSC, jun. 1990.
- [ 6 ] Hsu, C., "A Curvilinear-Coordinate Method for Momentum, Heat and Mass Transfer in Domains of Irregular Geometry," Ph.D. Thesis, University of Minnesota, USA, 1981.
- [ 7 ] Rhie, C.M., "A Numerical Study of the Flow Past an Isolated Airfoil with Separation," Ph.D. Thesis, University of Illinois, Urbana-Champaign, USA, 1981.
- [ 8 ] Peric, M., Kessler, R. and Scheuerer, G., "Comparison of Finite-Volume Numerical Methods with Staggered and Colocated Grids," Submitted to Computers and Fluids, 1987.
- [ 9 ] Bortoli, A.L., "The Use of Co-Located Variables

in the Solution of Supersonic Flows," (in portuguese), M.Sc. Dissertation, Federal University of Santa Catarina, Florianópolis, SC, Brazil, 1990.

- [10] Patankar, S.V., "Numerical Heat Transfer and Fluid Flow," McGraw-Hill, New York, 1980.
- [11] Harlow, F.H. and Welch, J.E., "Numerical Calculation of Time-Dependent Viscous Incompressible Flow of Fluid with Free Surface", Physics of Fluids, Vol. 8, pp. 2182-2189, 1965.
- [12] Silva, A.F.C. and Maliska, C.R., "Uma Formulação Segregada em Volumes Finitos para Escoamentos Compressíveis e/ou Incompressíveis em Coordenadas Generalizadas. Anais do II Encontro Nacional de Ciências Térmicas, p. 11-14, Aguas de Lindóia, Brasil, dez. 1988.
- [13] Van Doormaal, J.P. and Raithby, G.D., "Enhancements of the simple method for predicting incompressible fluid flows. Numerical Heat Transfer, Vol. 7, pp. 147-163, 1984.
- [14] Zedan, M. and Schneider, G.E., "3-D Modified Strongly Implicit Procedure for Finite Difference Heat Conduction Modelling," AIAA Journal, Vol. 21, n. 2, pp. 295-306, 1983.
- [15] ONERA, "Essai du Lanceur Bresilien au 1/15 Soufflerie S2MA; Configuration VC - C (5 dards), Mach 1.500, 2.502, 3.747," France, decembre 1988.